J Mater Sci (2007) 42:7566–7574
DOI 10.1007/s10853-007-1597-7

A simple synthesis of amine-derivatised superparamagnetic iron oxide nanoparticles for bioapplications

Sasmita Mohapatra · Nabakumar Pramanik · Samrat Mukherjee · Sudip K. Ghosh · Panchanan Pramanik

Received: 14 October 2006 / Accepted: 8 February 2007 / Published online: 24 May 2007

Abstract Adsorption of 3-aminopropyltriethoxysilane (APTS) on magnetite nanoparticles during its formation has been investigated to optimise the preparation of stable aqueous dispersion of amine derivatised magnetite nanoparticles. APTS adsorbs chemically on the surface of magnetite particle modifying its surface which is evident from thermal and C, H, N analysis. The variation of particle size has been observed with change of APTS concentration. X-ray diffractogram shows the formation of pure inverse spinel phase magnetite with average crystallite size 7 nm when equimolar (Fe_3O_4: APTS = 1:1) quantity of APTS was used during its synthesis. The presence of free surface $–NH_2$ groups and Fe–O–Si bonds was observed by FTIR. Raman spectrum further confirms the presence of surface $–NH_2$ groups. Transmission electron microscopy shows formation of particles of average size between 7 nm and 12 nm. The effective hydrodynamic diameter of the APTS coated particle agglomerates is 45.8 nm in stable aqueous colloidal dispersion, which is evident from photon correlation spectroscopy. VSM measurements at room temperature of both silanised and unsilanised magnetite shows their superparamagnetic nature with saturation magnetisation 41 e.m.u/g and 56 e.m.u/g, respectively. Avidin has been immobilised on the surface through glutaraldehyde, which demonstrates the possibility of the synthesised material to be used in protein immobilisation to form bioactive magnetic particles.

S. Mohapatra · N. Pramanik · P. Pramanik (✉)
Department of Chemistry, Indian Institute of Technology, Kharagpur, West Bengal, India
e-mail: pramanik06@gmail.com

S. Mohapatra
e-mail: sasmita@chem.iitkgp.ernet.in

S. K. Ghosh
Department of Biotechnology, Indian Institute of Technology, Kharagpur, West Bengal 721302, India

S. Mukherjee
UGC-DAE Consortium for Scientific Research, Kolkata 700091, India

Introduction

Study of bio-functionalised superparamagnetic iron oxide nanoparticles (SPION) is emerging as an interesting multidisciplinary area of research because of their potential applications in biology and medicine such as enzyme and protein immobilisation, magnetic resonance imaging (MRI), RNA and DNA purification, cell separation, targeted drug delivery and hyperthermia treatment [1–6]. The most important factor which influences the applicability of these magnetic particles is the successful attachment of biomolecules to the solid magnetic particle supports. As various biomolecules exhibit great diversities, a versatile approach of surface modification of the solid support is always required, which carefully balances the intermolecular forces between the molecules to be grafted and the outer layer of the solid support. In this context, surface modification with organosilanes is an interesting approach as these are compatible with many material used for biological purpose [7]. Organosilanes are bifunctional molecules having general formula $X\text{-}(CH_2)_n\ SiR_n(OR')_{3-n}$ where X = functional group and $–Si(OR)_n$ are anchoring groups by means of which they can be easily attached to the inorganic surfaces by forming strong Si–O–M bond (M is the metal from inorganic substrate) [8]. The most

common functional target for immobilizing protein molecules is the amine group, which is present on the vast majority of proteins due to the abundance of lysine side chain ε-amines and N-terminal α-amines. Though alkoxysilanes with various X (functionalities) are available, amino group is the most frequently used for biological purpose. The process of surface modification of iron oxides by silanisation is complex and depends upon a number of parameters like solvent type, temperature, and time as well as on the catalyst and type of concentration of organosilane used. The available literatures and patents describe silanisation of iron oxide after its synthesis [9–11]. But practically these naked magnetic particles heavily interact to agglomerate and form 200–400 nm clusters due to high dipole–dipole interaction [12]. Also the effects of various parameters like temperature, pH and silane concentration on surface functionalisation have been hardly considered. The optimisation of all these parameters is very much important to produce well-dispersed functionalised magnetic particles for subsequent tagging with biomolecules.

In this paper, amine derivatised magnetite nanoparticles have been synthesised in a single step by co-precipitation of Fe^{2+}/Fe^{3+} in presence of water-soluble 3-aminopropyltriethoxysilane (APTS). The quantity of surface adsorbed APTS during the formation of magnetite particle was determined by C, N and thermal analysis. The effect of APTS concentration of particle size and stability of the colloid was studied. The surface functional groups, structural purity, microstructure and magnetic property were studied by Fourier transform infrared spectroscopy (FTIR), Raman spectroscopy, X-ray diffraction (XRD) analysis, transmission electron microscopy (TEM), dynamic light scattering (DLS) and magnetisation by vibration sample magnetometry (VSM) respectively.

Materials and methods

Chemicals

All chemicals and reagents used were analytical grade and used without further purification. $FeCl_3$ and $FeSO_4 \cdot 6H_2O$ were obtained from Merck (Germany). 3-aminopropyltriethoxysilane was taken from Aldrich (USA). Millipore water was obtained from Milli-Q system (Millipore, Bedford, MA). Tetramethylrhodamine isothiocyanate (TRITC)-Avidin was taken from Sigma–Aldrich (USA).

Synthesis of APTS coated magnetite particles

Magnetite was synthesised according to the procedure developed by Massart [13, 14] with a little modification. In a 100 mL three naked flask equipped with a mechanical stirrer were taken 0.324 g of $FeCl_3$ and 0.278 g of $FeSO_4 \cdot 6H_2O$ in 40 mL of absolutely deoxygenated millipore water under argon. To the stirred reaction mixture variable amount of APTS (molar ratio of APTS: magnetite remains 1:4, 1:2, 1:1, 3:2, 2:1) was added over a period of 15 min during which a black precipitate formed, which spontaneously dissolved to give a clear solution. Black precipitate again reappeared by subsequent injection of 25% NH_3 solution. The reaction mixture was further stirred for 30 min. Then the particles were separated and washed five times with millipore using a magnetic concentrator.

Protein immobilisation study and determination of protein coupling efficiency

For activation of magnetic particles 1 mL of the particle suspension (50 mg/mL) was transferred to a 25 mL conical tube, washed with 0.01 M pyridine (pH 6.0) (4 × 5 mL) and incubated with 2 mL of 5% glutaraldehyde for 3 h at room temperature with vigorous shaking followed by washing with 0.01 M pyridine (2 × 5 mL). A total of 10 mg of protein (0.5 mg of Avidin-TRITC conjugate + 9.5 mg BSA) was taken in 1 mL 0.01 M pyridine. A total of 75 μL of this protein solution was added to 925 μL 0.01 M pyridine and kept as pre-coupling solution. Glutaraldehyde activated magnetic beads were incubated with about 75 μL protein solution for 16 h. The supernatant was removed magnetically, and saved as post-coupling solution. Then beads were washed with (3 × 100 μL) wash buffer (0.01 M Tris, 0.1% NaN_3, 0.1% w/v BSA, 0.1 M NaCl, 0.001 M EDTA, pH 7.4) magnetically and the supernatant added to the post coupling solution. The post coupling solution was made up to 1 ml by adding 0.01 M pyridine and saved for coupling efficiency determination. To the beads 5 mL 1 M glycine (quenching solution) was added and kept for 30 min. Avidin coupled magnetic beads were washed three times with washing buffer (0.01 M Tris, 0.1% NaN_3, 0.1% w/v BSA, 0.1 M NaCl, 0.001 M EDTA, pH 7.4). After washing particles were observed on glass slide under Leica Epi Fluorescent Microscope (DMR-MPS60). The same analysis was done with particles precipitated without using any silane.

Characterisation

The APTS concentration per gram of the dried particles was approximately estimated from C, H, and N analysis, using a Series II, Model 2400, Perkin Elmer, USA C, H, N analyzer.

The X-ray diffraction analysis was performed on the Phillips PW 1840 X-ray diffractometer after drying the samples prepared with different concentrations of APTS in vacuum. The lattice parameters were calculated by least

squares method and the crystallite size of the nano-crystalline samples obtained by X-ray line broadening analysis using Scherer's formula.

FTIR spectra of the prepared samples were done in KBr medium in the range 400–4,000 cm^{-1} with a model Thermo Nicolet Nexux FTIR (model 870).

Laser Raman Micro spectrometry was done with Renishaw Raman System 1000B coupled with a Leica DMLM microscope, using an argon laser with laser power 8 mW at the sample.

Thermal analysis (TG/DTG, DTA) was done with a thermal analyzer (Pyris Diamond TG/DTA) with a heating rate 8 °C per minute with in temperature range 50–850 °C.

TEM micrographs were obtained on a Phillips CM 200 transmission electron microscope with an acceleration voltage of 200 kV. The nanoparticles were thoroughly dispersed in water by ultra-sonication and placing a drop of solution on the carbon coated copper grid.

DLS analysis was done by taking one drop of aqueous suspension of as prepared nanoparticles in 10 mL millipore water by Brookhaven 90 plus particle size analyzer. The laser light of wavelength (λ = 660 nm) was scattered with an angle $\theta = 90°$ at 27 °C placing the dispersion in a polystyrene cuvette.

Room temperature magnetisation data of the freeze-dried samples were taken with magnetometer Lake Shore, Model-7410, USA.

Mössbauer measurements were carried out in the standard transmission mode by a PC based set-up working in the constant acceleration mode. ^{57}Co embedded in Rh matrix was used as the source. The Mössbauer data were deconvoluted using least squares fitting program.

Results and discussion

Two main steps involved in synthesis of nanocrystals by bottom-up method are (1) nucleation, (2) growth of nanocrystals. It is well known that the size of the nucleus is controlled by the solubility of the precipitate and super saturation of the reaction system.

The Fe_3O_4 magnetic nanocrystals are prepared by injecting NH_4OH to the mixture of Fe^{3+} and Fe^{2+}. A large amount of OH^- is added in order to increase the super saturation of the system. In fact, the ionic product of Fe^{2+} or Fe^{3+} and OH^- becomes much greater than solubility product, confirming the super saturation. The surface Fe atoms in magnetite are co-ordinatively unsaturated. As they carry unoccupied atomic orbitals, in aqueous systems they therefore co-ordinate with hydroxyl ions or water molecules which share their lone electron pair with Fe. Upon adsorption, the water molecules usually dissociate, resulting a surface covered by hydroxyl groups [15]. The silanol groups gradually formed by stirring APTS in acidic Fe^{2+}/Fe^{3+} solution are transformed to siloxane (Si–O–Si) bonds via condensation reaction at low pH [16]. Stirring the solution at high pH (9–10) for a long time, a coating of siloxane is formed through surface condensation on iron oxide surface [16].

The hydrodynamic diameter (HD) of the synthesised iron oxide particles prepared with increasing the concentration of APTS has been measured using DLS method. The intensity–intensity time correlation function has been accepted when the measured and calculated baselines are in good agreement. With increasing the amount of APTS the mean hydrodynamic diameter (MHD) calculated taking five consecutive effective HDs decreases, but after a certain concentration it again starts increasing (Fig. 1a). Aqueous naked Fe_3O_4 particles have tendency to agglomerate and form clusters as observed in case of AS-0 due to magnetic dipole interaction. But the use of APTS prevents the magnetic interaction and hence the particle-aggregate size decreases. But after a certain concentration of APTS again agglomeration is observed which can be explained on the basis of DLVO theory based on the consideration of balance between the molecular forces of attraction and ionic forces of repulsion that act between the particles. Coating of APTS on Fe_3O_4 reduces the possibility of adsorption of potential-determining ions (Fe^{2+}, Fe^{3+}, OH^-) on the surface. As a result the surface potential (φ_0) decreases. As the charge diminishes the electric force of repulsion between the particles weaken, particles stick together as they approach each other. At a sufficiently low $\varphi_{0\ crit}$ at which the energy barrier disappears and the thickness of $1/x$ (or h) of diffuse layers which surround the particles is expressed by the equation

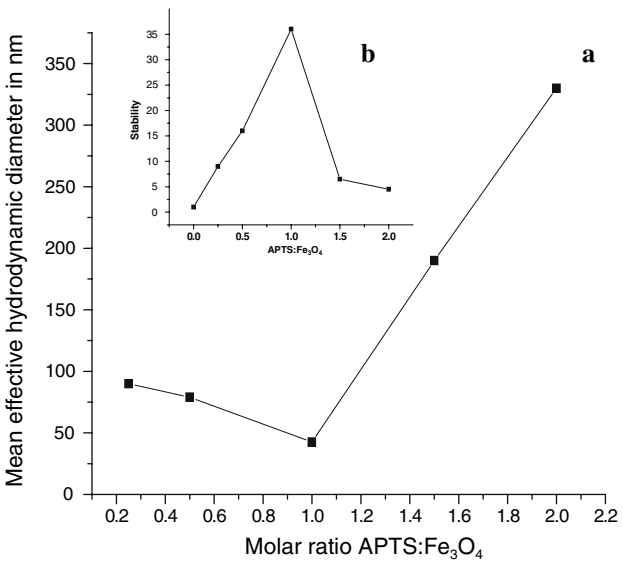

Fig. 1 Variation of MHD with of APTS conc

$$\varphi_{0,\text{critical}} = \sqrt{c\frac{A}{\varepsilon \cdot \frac{1}{x}}} = \sqrt{c\frac{Ax}{\varepsilon}}$$

where c = const.; A = attraction constant; ε = dielectric constant of the medium.

The relationship between $\varphi_{0\ \text{critical}}$ and x, which follows from the above equation has been empirically found by H. Eilers and J. Korff in 1936. According to them and the given equation

$$\Phi_0^2 h = C\frac{A}{\varepsilon} <> B$$

< B coagulation occurs; > B system is stable; B is a certain critical quantity and can be determined experimentally.

As more amount of APTS is adsorbed on Fe_3O_4 surface there is drop in Φ_0 potential and $\Phi_0^2 h < B$. Hence coagulation occurs. The effect of aminosilane concentration on the final product has been quantified in terms of its organic content and the density of surface $-NH_2$ groups (Table 1). It is clear that using equimolar amount of APTS as Fe_3O_4 (AS-3) the particle of minimum diameter has been obtained.

The X-ray diffraction patterns of the samples AS-0 and AS-3 are shown in Fig. 2. It is clear that there is no appreciable shift in peak position due to use of aminosilane. The lattice parameters calculated from least square method for both AS-0 and AS-3 are found to be 8.37 Å and 8.39 Å, respectively. The reported lattice parameter for inverse spinel magnetite is 8.37 Å. The *d*-values match well with that of inverse spinel magnetite (JCPDS card no 82-1533). The appearance of broad peaks indicates that both the samples are nano-crystalline in nature. The average mean crystallite sizes of all samples calculated taking into account the line broadening of each peak are given in Table 1.

The bright field TEM micrographs along with particle size distribution of AS-0 and AS-3 are presented in Fig. 3. AS-0 shows slight agglomeration, which may be due to the magnetic interaction of naked particles. It shows broad distribution of particles between 15 nm and 40 nm with a mean average particle size 25 ± 1 nm. AS-3 shows well dispersion of spherical particles and a significantly narrow particle size distribution between 7 nm and 12 nm. The mean average particle size is 9 ± 0.5 nm. It clearly indicates silanes/siloxanes prevent the growth of Fe_3O_4 nanoparticles by forming a thin coating on its surface. SAED pattern of AS-3 shows usual polycrystalline nature of the particles. The *d*-spacings calculated from electron diffraction accord with XRD. Figure 3c shows high resolution TEM of a single particle of AS-3 showing lattice imaging of [400] plane (d = 2.08 Å).

In order to verify the exact phase of the magnetite present Raman spectra was recorded with 10% laser power for 30 s integration time. Figure 4a presents the Raman spectrum of AS-3 between 200 cm^{-1} to 1,000 cm^{-1}. Though metal oxides are poor Raman scatterers, still Raman peaks of Fe_3O_4 and γ-Fe_2O_3 are sufficiently different to distinguish [17]. Less intense but distinct peaks at 684, 530 and 320 cm^{-1} correspond to magnetite core [18] and also it is further evidenced by Mössbauer study. The room temperature Mössbauer spectrum of the sample shows a doublet (Fig. 4b), which is typical of a sample undergoing superparamagnetic relaxation. The doublet was fitted with

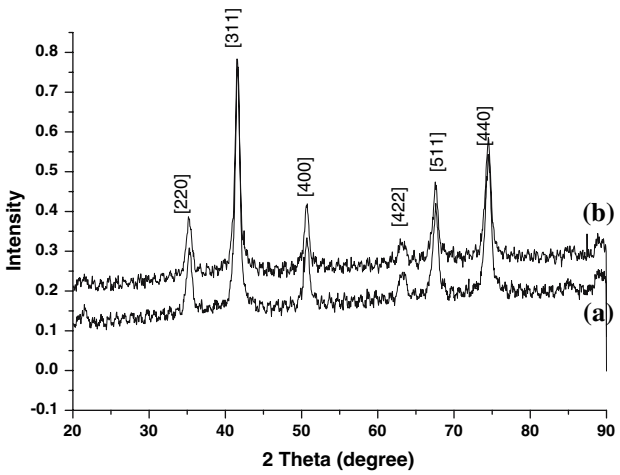

Fig. 2 X-ray diffractogram of (**a**) AS-0 (**b**) AS-3

Table 1 Physical properties of the samples prepared with varying Fe_3O_4: APTS ratio

Sample ID	APTS: Fe_3O_4	Hydrodynamic diameter (nm)	C, H, N (%)	Crystallite size (nm)	Surface $-NH_2$ groups (nmol/mg)	Stability (h)
AS-0	0.0	206	–	11.0	0	1.0
AS-1	0.25	90	1.46, 0.31, 0.465	10.9	10.5	9.0
AS-2	0.50	79	3.21, 0.928, 0.88	10.0	18.3	16
AS-3	1.0	45.8	4.45, 1.32, 1.50	7.0	32.4	36
AS-4	1.5	190	6.72, 1.93, 1.74	7.0	15.4	6.0
AS-5	2.0	330	8.72, 2.74, 2.62	6.5	11.2	4.5

a single symmetric doublet. The parameters obtained are given in Table 2. The isomer shift matches well with that reported by Hartridge et al. [19] thereby suggesting that the sample is nano-crystalline magnetite. The value of the quadruple splitting is slightly larger which may be due to the extremely small size of the particles in the sample. When the temperature of the sample is lowered down to 20 K, a clear sextet (Fig. 4c) is obtained which confirms the presence of superparamagnetism in the sample at room temperature. A single sextet was fitted to the spectrum, which is essentially two closely overlapping sextets arising from the A and the B sites of the spinel lattice. The isomer shift and the hyperfine field obtained matches well with that of magnetite. As mentioned, the slightly higher value of quadruple splitting is ascribed to the extremely small size of the sample.

The FTIR spectra of AS-3, AS-0 and APTS have been given in Fig. 5.1 and the corresponding band assignments are given in Table 3. In the FTIR spectrum of AS-3 absorption at 3,460 cm^{-1} and 1,625 cm^{-1} is due to O–H stretching and bending vibrations of physically adsorbed H_2O and surface –OH groups. Bands at 2,930 cm^{-1} and 2,853 cm^{-1} corresponds to $–CH_2–$ group of aminopropyl group attached to Si which are absent in AS-0. Bands at

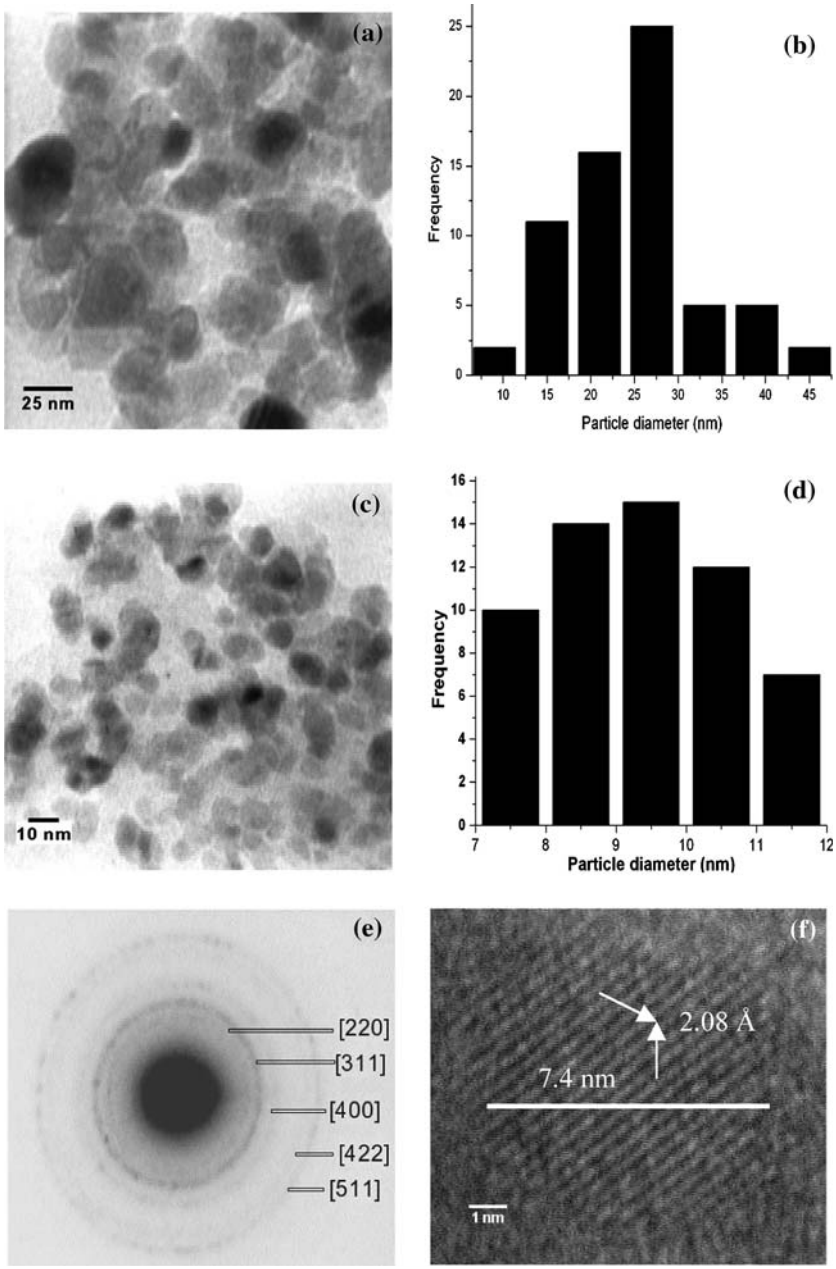

Fig. 3 (**a**) Transmission electron micrograph of AS-0 (**b**) Particle size distribution (**c**) Transmission electron micrograph 0f AS-3 (**d**) Particle size distribution of AS-3 (**e**) SAED pattern of AS-3 (**f**) HRTEM of a single particle of AS-3 showing the lattice imaging of [400] plane

1,123 $cm^{-1}$and 1,023 cm^{-1} contributed by C–N and Si–O bonds are not observed in the uncoated sample AS-0. For bulk Fe_3O_4 samples the vibration for Fe–O bond appears at 570 cm^{-1} and 375 cm^{-1}. But in this case there is blue shift to 670 cm^{-1} and 570 cm^{-1} due to size reduction [20]. Contributions from $–NH_2$ group were probably overlapped with that of vibration bands associated with water. To verify the presence of surface amino groups Raman spectrum was recorded at very low laser power (0.008 mw at sample for 300 s integration time). The Raman spectrum shows two distinct peaks at 3,220 cm^{-1} and 3,490 cm^{-1} (Fig. 5b), which may be attributed to $–NH_2$ and –OH peaks, respectively [21]. Thermal analysis (TG) further supports the presence of aminopropyl chain in the sample. Weight loss in APTS coated sample is in three stages (Fig. 6) which includes a small weight loss between 150 °C to 200 °C due to physically adsorbed water. Weight loss in between 300 °C and 400 °C is due to the loss of surface hydroxyl groups, which is present in both coated and uncoated samples (AS-0 and AS-3). Between 750 °C and 800 °C there is a small weight loss in AS-3, which is absent in uncoated sample AS-0, corresponds to the loss of organic moiety. This result shows that the APTS, which was used during precipitation of magnetite, forms a coating and is stable up to 750 °C. The density of the surface amine groups was measured using 4-nitrobenzaldehyde [22] and has been given in Table 1.

The magnetisation curves (Fig. 7) of both uncoated magnetite (AS-0) and silane coated magnetite (AS-3) show no hysteresis opening and are completely reversible at room temperature. Coercivity and remanence were not observed in both the samples, which indicate superparamagnetism. From M vs. 1/H plot the saturation magnetisation σ_s for uncoated magnetite is 56 e.m.u/g while that of coated particle is 41 e.m.u/g. Saturation magnetisation of bulk magnetite is 92 e.m.u/g. The decrease in saturation magnetisation of as prepared naked magnetite particles in comparison to bulk magnetite may be attributed to the decrease in particle size. It is reported in the literature that saturation magnetisation of ferrite nanoparticles decreases with decrease in particle size [12]. In addition, this decrease in saturation magnetisation may be due to different chemical composition on the surface like oxidation of Fe_3O_4 to Fe_2O_3, surface effect such as nonlinearity of spins of magnetically inactive layer with the magnetic field. Also the discrepancy could be explained by the variation in synthetic methods employed, which can generate particles

Table 2 The Mössbauer parameters obtained for AS-3

Sample temp (K)	Isomer shift (mm/s)	Quadruple splitting (mm/s)	Hyperfine field (T)
300	0.33	0.73	–
20	0.48	0.26	498

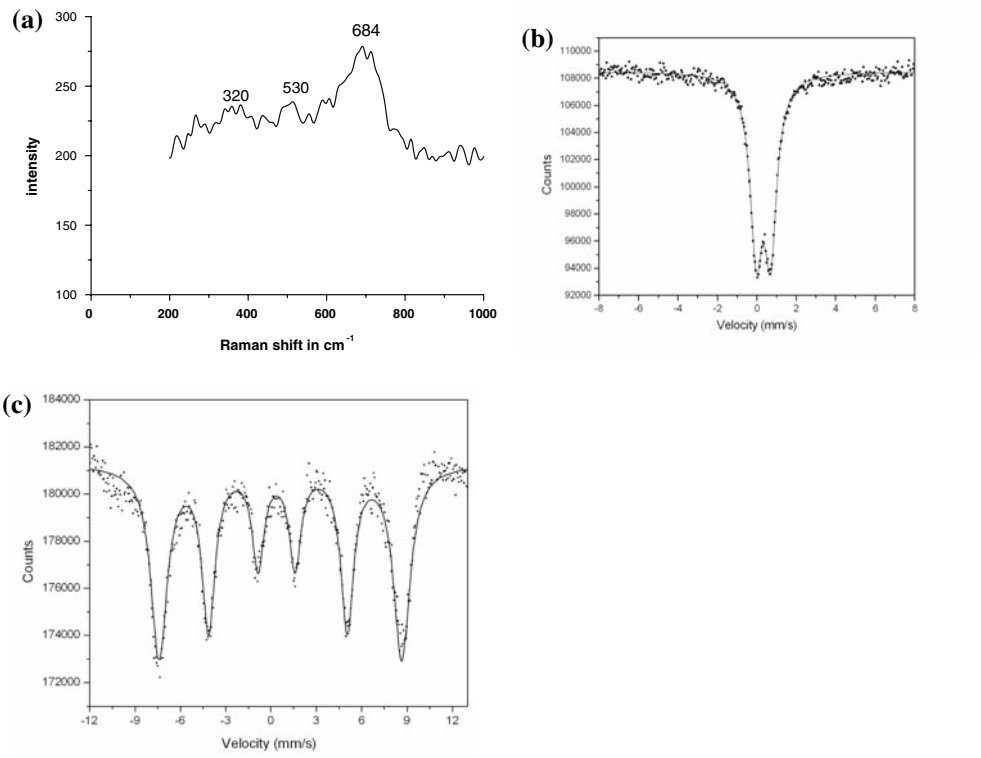

Fig. 4 (**a**) Raman spectrum of AS-3 at 0.08 mW laser power (**b**) Mössbauer spectrum of AS-3 at room temperature (**c**) Mössbauer spectrum of the same at 20 K

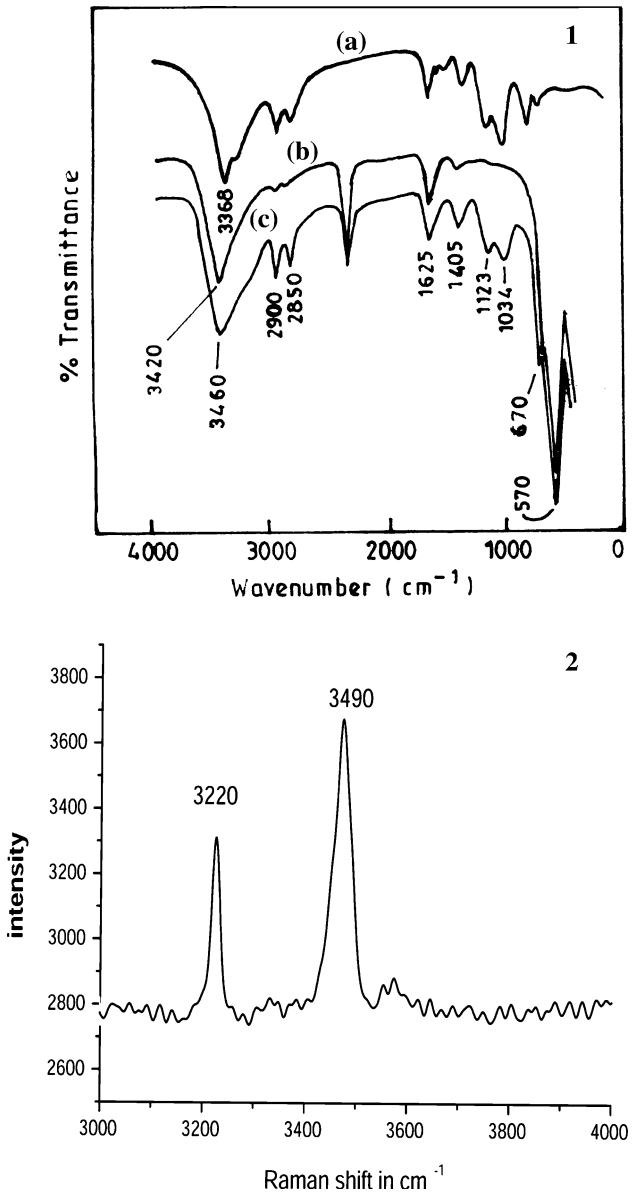

Fig. 5 (**1**) FTIR spectra of (a) APTS (b) AS-0 (c) AS-3 (**2**) Raman spectrum of AS-3 at 0.08 mW laser power

of different size. However, the saturation magnetisation value obtained here is consistent with the range of values reported in literature [23]. The saturation magnetisation of APTS coated magnetite particles (AS-0) is 41 e.m.u/g. This decrease in saturation magnetisation than naked as-prepared magnetite particles is an indication of formation of diamagnetic APTS coating contributes as a non-magnetic mass to the total sample volume, which is also supported by thermal analysis. Additionally a small decrease may be due to the detachment from dipole coupling due to well dispersion of APTS modified Fe_3O_4 particles. From slope of the magnetisation curve near H = 0, the magnetic particle diameter for both samples were calculated using the equation [24],

$$D_{mag} = \left[\frac{18kT\ (dM/dH)_0}{\Pi\rho M_S^2}\right]^{1/3}$$

where k is the Boltzmann constant, T is the absolute temperature, $[dM/dH]_0$ is the initial slope of the magnetisation curve near origin. ρ is the density of the Fe_3O_4(=5.24 g/cm^{-3}) [25]. The particle sizes calculated for uncoated (AS-0) and coated (AS-3) samples are 19 nm and 6.5 nm, respectively.

TRITC conjugated avidin was coupled with magnetic nanoparticles through glutaraldehyde. The quantitative adsorption of proteins on amine functionalised magnetite particles was determined in terms of its coupling efficiency. Coupling efficiency was obtained by measuring OD at 280 nm for both pre-coupling and post-coupling solutions and using the formula D = Dilution factor (=13.3).

$$\frac{[(OD_{280}\ \text{Pre - Coupling Solution} \times D) - (OD_{280}\ \text{Post - Coupling Solution} \times D)] \times 100}{OD_{280}\ \text{Pre - Coupling Solution} \times D)}$$

Table 3 Assignments of absorption bands in FTIR spectra

APTS (cm^{-1})	Fe_3O_4 coated with APTS (AS-3) (cm^{-1})	Uncoated Fe_3O_4 (cm^{-1})	Assignments
3368	–	–	ν^* NH···H
–	3420	3460	ν^* HO···H
			ν^* O···H
2942	2900	–	ν^*_{ass} CH···H
2874	2850		of $-CH_2$
1625	1625	1625	ν^*_{bend} O···H
1405	1405		δ^* C–OH
1123	1123	–	ν^* C···N
1070	1030	–	ν^* Si–O–Si
			Fe–O–Fe
–	578	575	ν^* Fe–O

ν^*, Stretching vibration; ν^*_{bend}, Bending vibration; δ^*, Deformation vibration; ν^*_{ass}, Asymmetric stretching

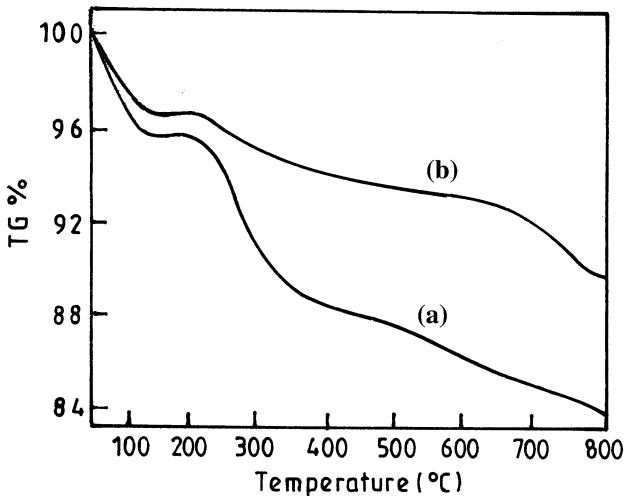

Fig. 6 TG curve of (**a**) AS-0 (**b**) AS-3

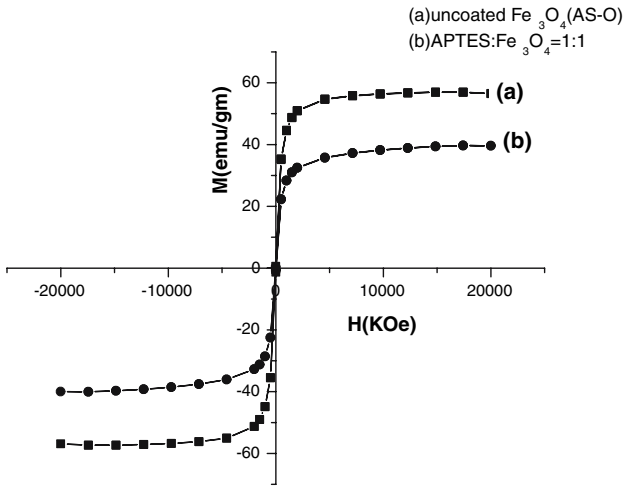

Fig. 7 Magnetisation curve of (**a**) AS-0 (**b**) AS-3

In this case coupling efficiency for TRITC conjugated avidin was found to be 73.5%. We have used TRITC conjugated avidin to visualise the conjugation under the fluorescent microscope (Fig. 8). Same approach can be taken to immobilise any other protein of interest like enzymes, antibodies etc. depending on the need. We have not found any binding with the uncoated magnetic nanoparticle. We have also immobilised a glycoprotein through glutaraldehyde with very high efficiency (82%) to these magnetic particles.

Conclusion

Superparamagnetic amine derivatised magnetite nanoparticles have been prepared in a single step at room temperature by simple co-precipitation method. The aminosilane concentration influences particle size. Particles of mean average size 9 ± 0.5 nm with high density of surface free $-NH_2$ have been obtained when molar ratio of Fe_3O_4:aminosilane was maintained as 1:1 in the reaction. Particle diameters calculated from different observations are reasonably in good agreement. Particles are highly hydrophilic and form stable aqueous suspension. Proteins, drugs and other bio-molecules can be attached through the surface amino group.

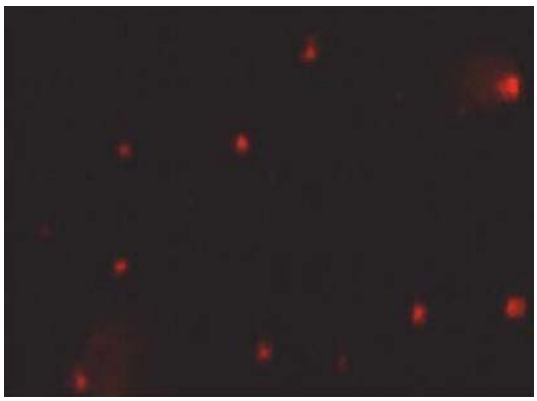

Fig. 8 Fluorescent micrograph of TRITC conjugated Avidin coated magnetite nanoparticles

Acknowledgements Authors are thankful to CSIR New Delhi for providing financial support for this work. Dr D. Das, IUC-DAE Consortium for Scientific Research, Kolkata, Dr M. K. Panigrahi, IIT Kharagpur and Dr D. Bahadur, IIT Bombay, Powai are gratefully acknowledged for Mössbauer, Raman and VSM studies, respectively.

References

1. Chaterjee J, Haik Y, Chen CJ (2001) J Magn Magn Mater 225:21
2. Bilková Z, Slováková M, Horák D, Lenfeld J (2002) J Chromatogr B 770:177
3. Pourfarzaneh M, Camel RS, London J, Dawes CC (1982) Method Biochem Anal 28:267
4. Homes E, Korsnes L (1990) Genet Anal Technol Appl 7:145
5. Sonti SV, Bose A (1991) J Colloid Inter Sci 170:575
6. Cupta PK, Hung CT (1989) Life Sci 44:175
7. Coradin T, Lopez PJ (2003) Chembiochem 4:251
8. Whitehead RA, Chagnon MS, Groman EU, Josephson L (1985) USP 4554,088
9. Ma M, Zhang Y, Yu W (2003) Colloids Surfaces A: Physicochem Eng Aspects 212(2–3):219
10. Yamaura M, Sampaio LC, Macêdo MA, Nakamura M, Toma HE (2004) J Magn Magn Mater 279(2–3):210
11. Shen X-C, Fang X-Z, Zhou Y-H, Liang H (2004) Chem Lett 33(11):1468–1469
12. Kobayashi H, Matsunaga T (1991) J Colloid Interface Sci 141:505
13. Massart R, Cabuil V (1987) J Chem Phys 84(7–8):967
14. Bee A, Massart R (1990) J Magn Magn Mater 122:1
15. Cornell RM, Schwertmann U (1996) The iron oxides: structure, properties, reactions, occurrence and uses. Wiley-VCH, Weinheim, p 207

16. Brinker CJ, Schere GW (1990) Sol–gel science: the physics and chemistry of sol-gel processing. Academic Press, Inc
17. Cornell RM, Schwertmann U (1996) The iron oxides: structure, properties, reactions, occurrence and uses. Wiley-VCH, Weinheim, p 135
18. De Faria LA, Venâncio Silva S, De Oliveria MT (1997) J Raman Spectroscopy 28:873
19. Hartridge A, Bhattacharya AK, Sengupta M, Majumdar CK, Das D, Chintalapudi SN (1997) J Magn Magn Mater 176:L89
20. Rao ZM, Wu TH, Peng SY (1995) Acta Phys Chim Sin 11:395
21. Mckittrick MW, Jones CW (2003) Chem Mater 15:1132
22. Bruce IJ, Sen T (2005) Langmuir 21:7029
23. Ambastha RD, Wattal PK, Singh S, Bahadur D (2003) J Magn Magn Mater 267:335
24. Bruke NAD, Stöver HDH, Dawson FP (2002) Chem Mater 14:4752
25. Cullity BD (1972) Introduction to magnetic materials. Addison-Wesley Publishing Company, p 190